# Modeling and Simulation of Deformable Elastic Body - Rigid Body Interaction

Mihai DUPAC

R&D Department
Haldex Corporation, Prattville, AL, USA
mihai.dupac@haldex.com

**Abstract.** In this paper a procedure for simulating deformable elastic body - rigid body interaction is presented. The interaction is described by multiple impacts during the dynamical process. An elastic body modeled as a 3D particles system is proposed, in response to the dynamic impacting force. The contact between particles is modeled with elastic springs. The expression for the spring elastic constants are presented. The force-deformation equation contains a damping term to reflect dissipation in the contact area. The procedure is applied to show interaction and deformation processes as well as realistic animations.
**Keywords**: Collision, Modeling, Impact, Computer graphics, Simulation
**Math. Subjects Classification 2000**: 70F35, 93A30, 74M20, 68U05, 68U20

## 1 INTRODUCTION

Modeling and simulation techniques are indispensable tools for the understanding of dynamical systems and a challenging subject in order to get a better understanding of their dynamical behavior.

Since realistic animation is a very important goal, numerous studies attempt to provide so-called "realistic method". Within these, the animation of elastic solids and their interaction is a difficult task due to the interaction conditions.

The interaction between bodies is a contact event (impact) that occurs at a common point or points of contact. Analytical solutions (obtaining post impact velocities in terms of pre-impact velocities) of rigid body collision problems in classical mechanics are formulated in terms of two principles: Newton's law of motion and Coulomb's law of friction. In addition, the solutions require the knowledge of two material constants: coefficient of friction and coefficient of restitution.

Multiple types of methods were proposed in order to predict the behavior after collisions. Kane and Levinson [8] showed that Newton's approach may predict erroneous energy results in rigid body problems when friction is present. Keller [9] formulated a three dimensional differential approach that resolved the energy paradox by using the kinetic definition of the coefficient of restitution.

An important recent contribution to the area was the energetic definition (a new coefficient of restitution) by Stronge [14] based on the internal dissipation hypothesis.

The collisions of kinematic chains with external surfaces were considered in Hurmuzlu and Chang [5]. They formulated an algebraic solution of impacts of planar multi-body system based on the kinematic formulation of the coefficient restitution.

Marghitu and Hurmuzlu [10] presented a three dimensional solution scheme based on the differential formulation of impact equations that incorporates three definitions of the coefficient of restitution. Dupac and Marghitu [6] studied rigid body collisions of planar kinematic chains with multiple contact points.

A molecular dynamics technique was used in [11] to describe particle interactions, for simulations of melting materials and viscous fluids.

In Desbrun and Gascuel [1] the SPH concepts were applied for the simulation of highly deformable bodies. Using a SPH particle-based method [12, 13], a 3D simulation for material properties ranging from highly plastic to stiff elastic was implemented.

A spring-particles model for melting solids with various forces applied to their neighbors was developed in Terzopoulos *et al.* [15]. A similar model using springs was developed in Dupac *et al.* [2].

The work in the present paper is dedicated for simulating a deforming elastic body - rigid body interaction.

For treating a moving and deforming elastic body in response to the dynamic force exerted by the interaction (impact) with a rigid body, an elastic body model is proposed. The elastic body is modeled as a 3D material particles. The contact between particles is modeled using elastic springs. Using a computational procedure developed in Dupac *et al.* [2] the spring elastic constants have been derived.

The external/internal forces (gravitational force, forces between particles, impulsive impacting forces), evaluated on each particle are presented. Furthermore to struggle out the local dynamics, the position and velocity of each particle is computed and continuously updated.

The advantage of the presented method is that enables accurate three-dimensional modeling, does not impose any modeling restrictions on the dynamic evolution of the system and has a very good computational time.

## 2 MECHANICAL MODEL OF THE DEFORMABLE ELASTIC BODY

For the study of the deformable elastic body - rigid body interaction a mechanical model is proposed. The deformable elastic solid considered for the simulation and shown in Fig. 1 is modeled as a mechanical system with particles in contact.

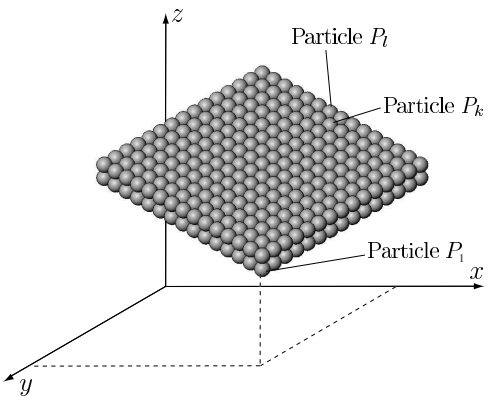


Fig. 1: Deformable elastic solid modeled as a system with particles in contact

The contact between particles is modeled using springs, resulting a lumped mass lumped spring model as shown in Fig. 2.

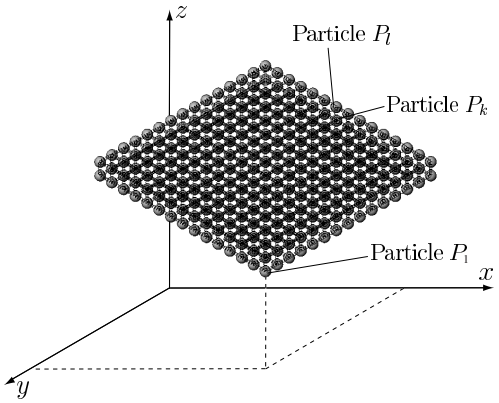


Fig. 2: Contact between particles modeled using springs

For the general case there are $n$ interconnected particles $P_1, ..., P_n$. The particles $P_j$, $j = l_1, l_2, \ldots, l_k$ with $l_i \in \{1, 2, ..., n\}$, $i = 1, 2, ..., k$ and $l_s \neq l_p$ for every $s \neq p$, may collide with the surface (rigid body) $S$. Each particle collision with surface $S$ leads to several outcomes depending on the initial conditions, the contact force and the coefficient of friction $\mu_j$ at the contact point among the surface. The contacting ends rebound as a result of the collision.

The center of the mass position of a particle $P_l$ with respect to the center of the mass position of a neighbor particle $P_k$ is shown in Fig. 3.

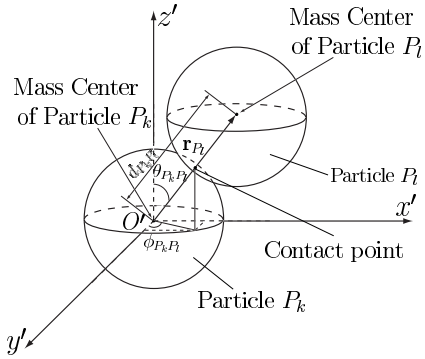


Fig. 3: Center of the mass position of a particle $P_l$ with respect to a neighbor particle $P_k$

For the moving reference frame $O'x'y'z'$ (Fig. 3.), the relative position of the particle $P_l$ with respect to the particle $P_k$ was described in a spherical coordinates system by $(d_{P_kP_l}, \phi_{P_kP_l}, \theta_{P_kP_l})$, where $d_{P_kP_l}$ represents the distance between the particles $P_k$ and $P_l$, $\phi_{P_kP_l}$ is the horizontal azimuth angle and $\theta_{P_kP_l}$ the azimuth angle.

The relations between Cartesian coordinates and spherical coordinates for the center of the mass of a particle $P_l$ with respect to the center of the mass of the neighbor particle $P_k$ can be written as

$$\begin{aligned} x'_{P_kP_l} &= d_{P_kP_l} \sin\theta_{P_kP_l} \cos\phi_{P_kP_l}, \\ y'_{P_kP_l} &= d_{P_kP_l} \sin\theta_{P_kP_l} \sin\phi_{P_kP_l}, \\ z'_{P_kP_l} &= d_{P_kP_l} \cos\theta_{P_kP_l}. \end{aligned}$$

The position vector of a particle $P_l$ with respect to the center of the mass of a neighbor particle $P_k$ can be expressed in the $O'x'y'z'$ cartesian reference frame as

$$\mathbf{r}'_{P_lP_k} = x'_{P_kP_l}\mathbf{i} + y'_{P_kP_l}\mathbf{j} + z'_{P_kP_l}\mathbf{k},$$

where $\mathbf{i}$, $\mathbf{j}$, $\mathbf{k}$ represents the units vector of the attached cartesian reference frame.

One can define the position of each particle $P_i$, $i = 2, ..., n$ in a fixed Cartesian reference frame $Oxyz$, using the position vector $\mathbf{r}_{P_1} = \lambda_x\mathbf{i} + \lambda_y\mathbf{j} + \lambda_z\mathbf{k}$ of the particle $P_1$, and the position vectors $\mathbf{r}'_{P_lP_{l+1}}$, $l = 1, 2, ..., i-1$. One can write

$$\mathbf{r}_{P_i} = \mathbf{r}_{P_1} + \sum_{l=1}^{i-1} \mathbf{r}'_{P_lP_{l+1}}.$$

For the previous relation, the fixed reference frame $Oxyz$ is parallel, i.e. $Ox \| O'x'$, $Oy \| O'y'$ and $Oz \| O'z'$, and have the same orientation with the moving reference frame $O'x'y'z'$ attached to each particle.

The velocity vector $\mathbf{v}_{P_i}$ of the particle $P_i$, $i = 2, ..., n$ is the derivative with respect to time of the position vector of $\mathbf{r}_{P_i}$, $\mathbf{v}_{P_i} = \dot{\mathbf{r}}_{P_i}$. The acceleration vector $\mathbf{a}_{P_i}$ of the particle $P_i$, $i = 2, ..., n$ is the derivative with respect to time of the position vector of $\mathbf{r}_{P_i}$.

The evolution of the system is governed by the fundamental law of dynamics,

$$\mathbf{F}_{P_i} = m_{P_i}\mathbf{a}_{P_i}, \tag{1}$$

where $m_{P_i}$ is the mass of each particle $P_i$ and $\mathbf{a}_{P_i}$ is its acceleration caused by the force $\mathbf{F}_{P_i}$. The force $\mathbf{F}_{P_i}$ can be divided between the internal and external forces.

The internal force $\mathbf{F}_{P_i}^{int}$ is the resultant of the tensions of the springs linking the particle $P_i$ to its neighbors

$$\mathbf{F}_{P_i}^{int} = \sum_{j \neq i} k_{ij}^{c} [\frac{\|\mathbf{r}_{P_i P_j}\| - l_{P_i P_j}}{\|\mathbf{r}_{P_i P_j}\|}]\mathbf{r}_{P_i P_j}, \tag{2}$$

where $k_{ij}^{c}$ and $l_{P_i P_j}$ are, respectively, the stiffness and the rest length of the spring linking the particle $P_i$ with the particle $P_j$.

The external force depends to the kind of load to which the model is exposed. Omnipresent loads will be gravity, contact (impact) forces, and damping. The role of the damping is to model the dissipation of the mechanical energy of the model.

The gravitational force acting on the particle $P_i$ is given by

$$\mathbf{G}_{P_i} = m_{P_i}\mathbf{g}, \tag{3}$$

where $\mathbf{g}$ is the gravitational acceleration.

The vector of contact forces is given by

$$\mathbf{F} = \left\{F_1^t, F_1^n, \ldots, F_k^t, F_k^n\right\}^T, \tag{4}$$

where, $F_j^n$ is the normal contact force and $F_j^t$ is the tangential contact force. The impulses at the contact points are obtained by integrating Eq. (4), which gives:

$$\tau = \begin{bmatrix} \tau_1^t \\ \tau_1^n \\ \vdots \\ \tau_k^t \\ \tau_k^n \end{bmatrix} = \begin{bmatrix} \int_0^t F_1^t dt \\ \int_0^t F_1^n dt \\ \vdots \\ \int_0^t F_k^t dt \\ \int_0^t F_k^n dt \end{bmatrix}, \tag{5}$$

where,

$$\tau_j = \tau_j^t \mathbf{t}_j + \tau_j^n \mathbf{n}_j, \quad (j = 1, ..., k), \tag{6}$$

where $\mathbf{n}_j$ is the unit vector normal to the impacting surface, and $\mathbf{t}_j$ the unit vector in the common tangent plane and satisfying $\mathbf{n}_j = \mathbf{t}_j \times \mathbf{k}$.

## 3 SPRINGS STIFFNESS

For the derivation of the spring constants a procedure developed in Dupac *et al.* [2] and briefly described below is used.

For the particles-springs model (Fig. 1), the particles are considered to be spheres with the same radius $r_0$, and are connected only with the neighbor particles (the contacts between particles are modeled through linear springs).

The average stress tensor for a 3D assembly of particles can be expressed as

$$\sigma_{ij} = \frac{M}{2V} \sum_{\phi} \sum_{\theta} b_i^c(\phi,\theta) f_j^c(\phi,\theta) f(\phi,\theta) \sin\phi \Delta\phi \Delta\theta, \tag{7}$$

where $m_{P_i}$ is the mass, and $V^{P_i}$ is the volume of the particle $P_i$, $M$ is the mass and $V$ is the volume of the assembly, $b_i^c(\phi,\theta)$ are the value of the vectors that connect the centers of particles in contact, and $f_j^c(\phi,\theta)$ are the contact forces at the solid angle defined by $\theta$ and $\phi$ as shown in Fig. 4.

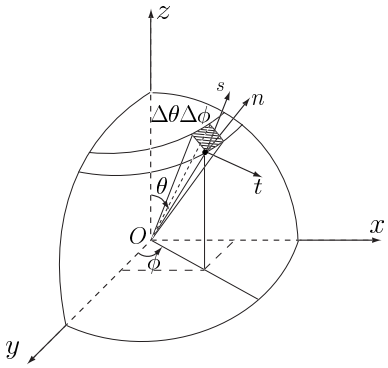


Fig. 4: Solid angle for the particles in contact

Using Hooke's low, the contact force is defined as $f_j^c = k_{ij}^c \Delta_j^c$, where $k_{ij}^c = k_n n_i n_j + k_s s_i s_j + k_t t_i t_j$ spring constant, $k_n$, $k_s$, $k_t$ are the normal and tangential stiffness at contact,

$$n = (\cos\phi \sin\theta, \sin\phi \sin\theta, \cos\theta)$$

and

$$s = (-\sin\phi, \cos\phi, 0), t = (\cos\phi\cos\theta, \sin\phi\cos\theta, -\sin\theta)$$

are the normal and tangential unit vectors as shown in Fig. 4.

The strain-displacement relation for a particle at the contact point is $\Delta_m^c = \varepsilon_{ml} b_l^c$, where $\varepsilon_{ml}$ is the strain tensor of the assembly. The relation between strain tensor $\varepsilon_{kl}$ and the stress tensor $\sigma_{ij}$ can be expressed as $\sigma_{ij} = A_{ijml}\varepsilon_{ml}$. The effective elastic stiffness tensor $A_{ijml}$,

$$A_{ijml} \simeq \frac{r_0^2 M}{2\pi V} \int_0^{2\pi} \int_0^{\pi} (k_n n_i n_j n_m n_l + k_s n_i s_j s_m n_l + k_t n_i t_j t_m n_l) \sin\phi \mathrm{d}\phi \mathrm{d}\theta.$$

was obtained using $f(\phi,\theta)=\dfrac{1}{4\pi}$ and $b_i^c=(2r_0)n_i$ and by replacing the summation with integration.

Using the symmetric condition $\sigma_{ij}=\sigma_{ji}$ for stress, and $\varepsilon_{ij}=\varepsilon_{ji}$ for strain, the previous integral can be replaced by a matrix formulation.

From continuum mechanics, using the relations between the state of stress and strain defined for an isotropic material, and the engineering shear strain properties, the stiffness can be written as

$$k_n=\frac{3}{2}\frac{EV}{Mr_0^2(1-2\nu)},$$
$$k_s=\frac{3}{2}\frac{EV(4\nu-1)}{Mr_0^2(2\nu^2+\nu-1)},$$
$$k_t=\frac{3}{2}\frac{EV(4\nu-1)}{Mr_0^2(2\nu^2+\nu-1)},$$

where $E$ is the Young's modulus and $\nu$ is the Poisson's ratio of the material (for more details about the stiffness computation see Dupac *et al.* [2]).

## 4 COLLISION RESPONSE

The normal impulsive forces, $F_j^n$, $j=1,2,\ldots,k$, are determined by combining the classical Hertzian contact theory (Goldsmith [4]) and elastic-plastic indentation theory (Johnson [7]). At a contact point there is a linear relationship between the plastic deformation $q_{pj}$ and the normal contact force $F_j^n$, as follows

$$q_j^p=\eta(F_j^n-F_j^c). \tag{8}$$

In the above equation the coefficient $\eta$ has the following expression

$$\eta=\frac{1}{2\pi R_j H}, \tag{9}$$

where $H$ characterizes the plastic property of the material and can be approximate with the Brinell hardness, and $R_j$ is the radius of the impacting particle. The critical value of the impact force $F_j^c$, can be expressed in terms of the yield stress $\sigma_y$

$$F_j^c=\frac{8\pi^3R_j^3\sigma_y^3}{k_1^2}, \tag{10}$$

where

$$k_1=\frac{2}{3(1-\nu^2)}E\sqrt{R_j}. \tag{11}$$

The elastic deformation $q_j^e$ as a function of the contact force is described by the Hertz's law

$$q_j^e=\left(\frac{F_j^n}{k_1}\right)^{2/3}, \tag{12}$$

and the total normal deformation for the elasto-plastic impact is the sum of elastic and plastic deformation

$$q_j = q_j^e + q_j^p = \left(\frac{F_j^n}{k_1}\right)^{2/3} + \eta(F_j^n - F_j^c). \tag{13}$$

The critical deformation $q_j^c$ corresponds to the force $F_j^c$, and the maximum deformation $q_m$ appears when the maximum force $F_j^m$ is applied. The impact force at the impact point is

$$\mathbf{F}_j = F_j^n \mathbf{n} + F_j^t \mathbf{t}, \tag{14}$$

where $F_j^t$ is the friction force.

## 5 IMPLEMENTATION AND RESULTS

The procedure for simulating deformable elastic body - rigid body interaction was implemented for the case of a rubber sheet. When the rubber sheet is released, the distance between the rubber sheet and cylinder is $d = 0.25$ m. The rubber sheet has the length $l = 0.15$ m, the width $d = 0.15$ m, and the height $h = 0.015$ m. The elastic properties for the rubber sheet are: elastic modulus $E = 6100000$ N/m$^2$, Poisson ratio $\nu = 0.49$, shear modulus 2900000 N/m$^2$ and a mass density of $\rho = 1000$ Kg/m$^3$. The coefficient of static friction is $\mu_s = 0.7$ and the coefficient of dynamic friction is $\mu_k = 0.57$. The gravitational acceleration $g = 9.807$ m/s$^2$ is considered.

In Fig. 5 the 3D particle rubber sheet model in the moment of impacting the cylinder is presented.

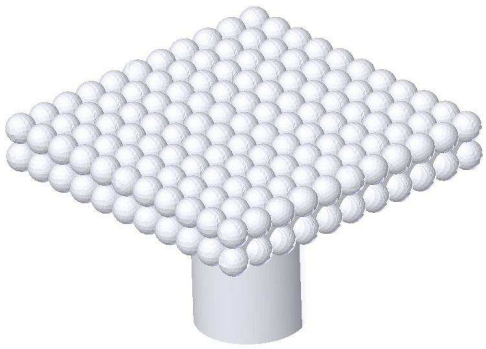

Fig. 5: Simulated 3D particle model of a rubber sheet immediately before impacting a cylinder

A snapshot of the dynamic deformation of the 3D particle model of a rubber sheet after impacting the cylinder is presented in Fig. 6.

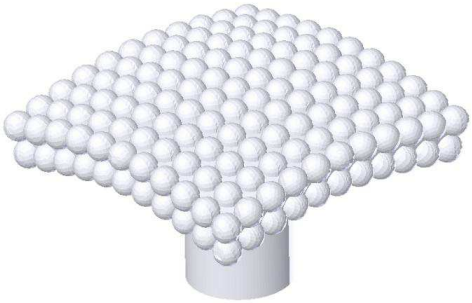

Fig. 6: Simulated 3D deformed particle model of a rubber sheet after impacting a cylinder

For the deformation associated with Fig. 6, it was observed that all the springs have a reasonable deformation rate. Regarding the animation sequence, the amplitude of the oscillation of the falling sheet after the impact dissipate very quickly due to the computed springs constants. By changing the damping coefficient, the oscillations of the sheet can be modified in order to obtain a better and more "realistic" animation.

The deformation of rubber sheet was verified using a FEM model, a well established engineering method. The FEM model was developed for both static and dynamic systems based on elastic theory and finite element principles. The FEM model of the rubber sheet in the moment of impact is presented in Fig. 7.

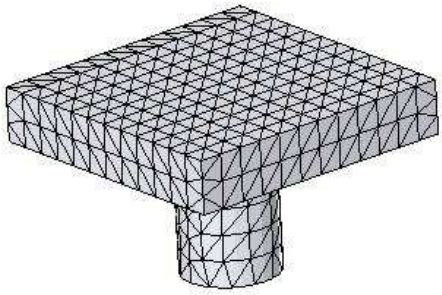

Fig. 7: Simulated 3D FEM model of a rubber sheet immediately before impacting a cylinder

Fig. 8 presents a snapshot of the dynamic FEM simulation, the deformation of the rubber sheet after impacting the cylinder.

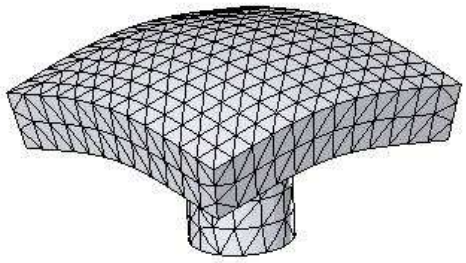

Fig. 8: Simulated 3D deformed FEM model of a rubber sheet after impacting a cylinder

The same deformation was observed in both simulation, so the spring model was considered to be accurate.

The interaction and deformation behavior performed using the 3D spring modeling is a low cost dynamic procedure. At a given stiffness the computational cost of the 3D particle model algorithm is lower than that of the FEM elastic model. Therefore, the spring algorithm is faster that the classic FEM algorithm.

## 6 CONCLUSIONS

In this work, the modeling, simulation and visualization of an deformable elastic body - rigid body interaction phenomena, has been considered. The elastic solid, modeled as a 3D particles system have been considered. The contact between particles has been simulated by elastic springs. The expression for the spring elastic constants have been presented.

The external/internal force have been evaluated on each particle, and the associated boundary conditions imposed. The collision techniques are based on the differential formulation of the equations of impact with the normal impulsive forces determined by combining the classical Hertzian contact theory and elastic-plastic indentation theory. The model was verified using a FEM based model.

## References

[1] **M. Desbrun and M. P. Gascuel** , Smoothed particles: A new paradigm for animating highly deformable bodies, *Computer Animation and Simulation*, Vol. 96, 1996, p. 61-76.

[2] **M. Dupac, D. G. Beale and R.A. Overfelt** , Three-Dimensional Lumped Mass/Lumped Springs Modelling and Nonlinear Behavior of a Levitated Droplet, *Nonlinear Dynamics*, Vol 42,(1), 2005, p. 25-42.

[3] **R. Gingold and J. Monaghan**, Smoothed particle hydrodynamics - theory and application to nonspherical stars, *Monthly Notices of the Royal Astronomical Society,* Vol. 181, 1977, p. 375-389.
[4] **W. Goldsmith**, (Eds.), Impact, Edward Arnold Publishers Ltd., London, 1960.
[5] **Y. Hurmuzlu and T. Chang**, Rigid Body Collisions of a Special Class of Planar Kinematic Chains, *IEEE Transaction in System, Man, and Cybernetics*, Vol. 22,(5), 1992, p. 964-971
[6] **M. Dupac and D. B. Marghitu**, Open Kinematic Chains with Multiple Impacts, *Proceeedings of the Thirteenth International Congress on Sound and Vibration, ICSV13* - Vienna, Austria, 2006 (accepted)
[7] **K. L. Johnson**, Contact Mechanics, Cambridge University Press, Cambridge, 1985
[8] **T. R. Kane and D. A. Levinson**, Dynamics: Theory and Applications, McGraw-Hill, New York, 1985
[9] **J. B. Keller**, Impact with Friction, *ASME Journal of Applied Mechanics*, Vol. 53, 1986, p. 1-4
[10] **D. B. Marghitu and Y. Hurmuzlu**, Three Dimensional Rigid Body Impact with Multiple Contact Points, *ASME Journal of Applied Mechanics*, Vol. 6, 1995, p. 725-732
[11] **G. Miller and A. Pearce**, Globular dynamics: A connected particle system for animating viscous fluids, *Computers & Graphics*, Vol. 13,(3), 1989, p. 305-309
[12] **M. Muller, D. Charypar and M. Gross**, Particle-based fluid simulation for interactive applications, *SIGGRAPH/Eurographics Symposium on Computer Animation*, 2003, p. 154-159.
[13] **M. Muller, R. Keiser, A. Nealen, M. Pauly, M. Gross and M. Alexa**, Point based animation of elastic, plastic and melting objects, *SIGGRAPH/ Eurographics Symposium on Computer Animation*, 2004, p. 141-151
[14] **W. J. Stronge**, Rigid Body Collisions with Friction, In *Proceedings of Royal Society*, London, Vol. A 431, 1990, p. 169-181
[15] **D. Terzopoulos, J. Platt and K. Fleischer**, Heating and melting deformable models (from goop to glop), *Graphics Interface*, 1989, p. 219-226